Working Formula for Precise Calculation of the Electric Field in a Microchannel

Yong Kweon Suh¹, Seong Gyu Heo¹ & Sangmo Kang¹

¹Department of Mechanical Engineering, Dong-A University, 840 Hadan-dong, Saha-gu, Busan 604-714, Korea Correspondence and requests for materials should be addressed to Y.K. Suh (yksuh@dau.ac.kr)

Accepted 22 March 2007

Abstract

In this paper, we present a working formula for calculating the electric field inside a microchannel that has two reservoirs, one attached at either end of the channel, supplying the electric charge. For the case where the channel width is much smaller than the reservoir size, as is usually the case, we designed a method to patch the numerical solutions obtained for the reservoir domain and the asymptotic solutions valid for the region near the entrance to the channel where it attaches to the reservoir. Assuming small channel size, we also derived two asymptotic solutions, for the potential and for the electric field applicable to the reservoir and to the channel regions. A working formula was then established that could predict the effects of the electrode and channel size relative to the reservoir on the electric field built inside the channel. The working formula was robust and applicable to a wide range of parameter values.

Keywords: Microchannel, Entrance effect, Electric field, Asymptotic solutions

Introduction

Recently, there has been a great deal of interest in microfluidics. In particular, microchannels have frequently been utilized to convey a liquid from one place to another. As for the fluid-driving force, electro -osmotic force has been used predominantly among other tools such as pressure force¹. To generate an electro-osmotic force, the channel is connected to two reservoirs, one at either end, in which electrodes are submerged. As soon as a certain electric-potential difference is applied between the two electrodes, an

almost constant electric field is generated within the channel. The ionic molecules (positively charged) within the EDL (Electric Double Layer) very near the channel wall are then driven toward the cathode by this electric field¹.

The driving velocity is proportional to the local electric field at the channel wall². In most cases, this electric field is obtained by dividing the applied potential difference by the channel length, irrespective of the reservoir design. However, because the two electrodes are usually situated at the center of the corresponding reservoir, the electric potential at the end of the channel is not the same as that of the electrode itself. So, we may expect that the electric field calculated conventionally may over-predict the actual true electric field. To our knowledge, there have been no studies on the effect of the channel entrance on the electric potential and the electric field.

In this paper, we propose a working formula to predict the effect of electrode size and channel width relative to reservoir size on the electric field built up within the channel. To solve the Laplace equation for the electric potential, we used the finite difference method after conformal mapping of the coordinates. The boundary condition at the interface of the channel was supplied from the asymptotic solution obtained near the channel entrance. On the other hand, two analytic solutions were also derived that are asymptotically correct for small electrode and channel sizes, one for the reservoir and the other for the channel region. These solutions, together with the numerical results, were then used to derive a working formula to predict the electric field built up inside the channel.

In the next two sections of this paper, we will derive the asymptotic solutions for the potential, one for the reservoir and the other for the channel entrance region, assuming small electrode and channel size; the next section will describe the numerical method for solving the Laplace equation for the potential within the reservoir; then, after the numerical results are presented, the working formula will be derived to predict the electric field inside the channel.

Asymptotic Solutions for the Potential in the Reservoir

The fundamental problem we considered in this paper was to find an electric potential within a geo-

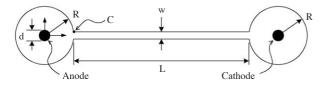


Figure 1. Microchannel connecting two circular reservoirs that contain electrodes.

metry composed of two circular reservoirs of radius R, each with an electrode of diameter d at its center, and the connecting channel of width w (Figure 1). Without loss of generality, we can take R=1. The center of the electrode's anode is considered the origin of the Cartesian coordinates (x, y), as shown in Figure 1. As the problem has symmetric properties, we confined ourselves to the upper half-plane, $y \ge 0$. The governing equation for the electric field is the Laplace equation¹,

$$\nabla^2 \phi = 0 \tag{1}$$

All the surrounding boundaries, except the electrode surface, are insulated.

Assuming that both the electrode diameter and the channel width are very small compared to the reservoir size, we can obtain the asymptotic solution of the Laplace equation (1) for the potential that is relevant to the region within the reservoir. For this, we first introduce a conformal mapping:

$$z = \exp(\rho) \tag{2}$$

where z=x+iy is the complex Cartesian coordinate and $\rho=\xi+i\eta$ is the transformed coordinate (Figure 2b). The cylindrical coordinates are $r=exp(\xi)$ and $\theta=\eta$. Then, using the Schwarz-Christoffel transformation method^{3,4}, we can transform the ρ -plane to the σ -plane on which the boundary is now flat, as shown in Figure 2(c). The relationship between the two planes is

$$\sigma = -\cosh\rho \tag{3}$$

in which $\rho=0$, $\sigma=-1$ at point B, and $\rho=\pi i$, $\sigma=1$ at point D. Since point B is considered a sink for the electric field, the complex potential W= $\phi+i\psi$ is given by

$$W = \frac{m}{2\pi} \ln(1 + \sigma) \tag{4}$$

where m is the total flux of the electric field:

$$\mathbf{m} = \int_{\mathbf{A}} \mathbf{E} \cdot \mathbf{d} \mathbf{A}$$

Here, E is the electric field vector, and the cross-sec-

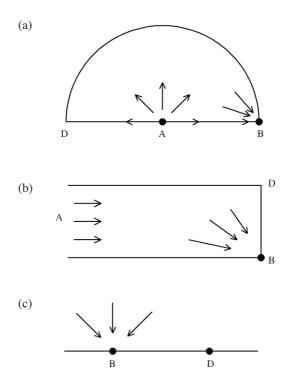


Figure 2. Sketches of the physical plane (a), the transformed ρ -plane (b) and the transformed σ -plane (c) used to derive the asymptotic solution of the Laplace equation for potential in the circular reservoirs.

tional area **A** covers not only the upper half-plane, $y \ge 0$, but also the lower half-plane, y < 0 on the electrode surface; within the channel, it covers the whole channel width. The quantity m can also be considered the total electric charge divided by the electric permittivity of the medium inside the domain. By substituting (3) and (2) into this equation, we can write the complex potential in terms of the physical coordinates as follows:

$$W = \frac{m}{2\pi} \ln[1 - (z + 1/z)/2]$$
(5)

The electric potential is given by ϕ =Real(W), and its conjugate pair by ψ =Im(W).

Figure 3 shows the equi-potential lines and the electric field lines obtained with (5). It can be shown that $\psi=0$ on the outer wall of the reservoir and that $z=\exp(i\eta)$.

Asymptotic Solutions for the Potential near the Channel Entrance

Assuming that the channel size is very small compared to the reservoir size, we can approximate the region very close to the channel entrance as the one shown in Figure 4(a). To obtain the solution for the

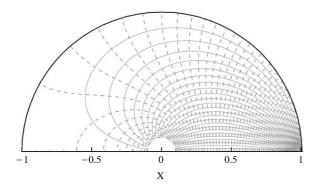


Figure 3. The equi-potential lines (dashed) and electric field lines (solid) obtained from the asymptotic solution (5) with m=1. The increment of both contour levels is 0.02.

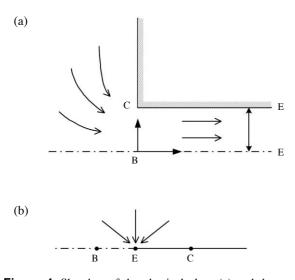


Figure 4. Sketches of the physical plane (a) and the transformed ζ -plane (b) used to derive the asymptotic solution of the Laplace equation for potential in the channel.

Laplace equation with this geometry, we use the Schwarz-Christoffel transformation method^{3,4}:

$$\frac{\mathrm{d}z_1}{\mathrm{d}\zeta} = \mathrm{Ki}\frac{\sqrt{1-\zeta}}{\zeta} \tag{6}$$

where $z_1 = (x-1) + iy$ is the physical plane shifted from z, and ζ is the transformed plane (Figure 4(b)). The constant K is evaluated from a matching condition for a specific point in both planes, i.e., z_1 and ζ . Integrating and applying the conditions for point C, i.e.,

$$z_1 = \frac{w}{2}i$$
 at $\zeta = 1$

we obtain the following relationship:

$$z_{1} = -\frac{W}{\pi} \left(\sqrt{1 - \zeta} + \frac{1}{2} \ln \frac{\sqrt{1 - \zeta} - 1}{\sqrt{1 - \zeta} + 1} \right)$$
(7)

For a given z_1 , we apply the Newton-Rhapson method to obtain ζ from this equation. Then, the complex potential is given by

$$W = \frac{m}{2\pi} \ln \zeta \tag{8}$$

where m denotes the total strength of the sink. Here, too, m covers both the upper half-plane, $y \ge 0$, and the lower half-plane, y < 0. The electric potential is in turn given by

$$\phi = \frac{m}{2\pi} \operatorname{Real}[\ln \zeta] \tag{9}$$

The complex electric field can be obtained from

$$\frac{\mathrm{dW}}{\mathrm{dz}} = -\frac{\mathrm{m}}{\mathrm{w}} \frac{1}{\sqrt{1-\zeta}} \tag{10}$$

and the x-component of the electric field by

$$\mathbf{E}_{\mathbf{x}} = -\frac{\partial \phi}{\partial \mathbf{x}} = \frac{\mathbf{m}}{\mathbf{w}} \operatorname{Real}\left[\frac{1}{\sqrt{1-\zeta}}\right] \tag{11}$$

Numerical Method for the Electric Potential in the Reservoir

The governing equation (1) is solved numerically in the ρ -plane with the following boundary conditions:

$$\phi = 1$$
 at $\xi = \xi_a$ (12a)

$$\phi = \phi_b(\eta) \text{ at } \xi = \xi_b \text{ for } 0 \le \eta \le \eta_c$$
(12b)

$$\frac{\partial \phi}{\partial \eta} = 0 \text{ at } \eta = 0, \pi$$
 (12c)

$$\frac{\partial \phi}{\partial \xi} = 0 \text{ at } \xi = \xi_b \text{ for } \eta_c \le \eta \le \pi$$
 (12d)

where $\xi_a = \ln(d/2)$ and $\xi_b = \ln(R) = 0$ represent the ξ coordinate at the electrode surface and the outer wall of the reservoir, respectively, and $\eta_c = \tan^{-1}(w/2R)$ is the η coordinate of the corner point C. The function $\phi_b(\eta)$ is an electric potential function given from the asymptotic solution for the channel, i.e., (9), with $\phi_b(\eta_c)=0$ for a specific m value dictated by the numerical solution. A more detailed explanation of this will be given later.

The governing equation (1) together with the boundary conditions (12a)-(12d) is discretized by the central difference algorithm with uniform grids in the ρ plane. In discretizing the Neumann-type boundary conditions (12c) and (12d), we used a second-order difference formula. For instance, the normal derivative $\partial \phi / \partial \xi$ on the outer wall can be expressed in terms of the boundary value ϕ_1 at $\xi=0$ and its neighboring values ϕ_2 at $\xi=-\Delta \xi$ and ϕ_3 at $\xi=-2\Delta \xi$, with

$$\frac{\partial \phi}{\partial \xi} = \frac{4\phi_2 - \phi_3 - 3\phi_1}{2\Delta\xi} \tag{13}$$

The algebraic equation obtained after discretization is then solved using the ICCG (Incomplete Cholesky Conjugate Gradient) method^{5.6}, using grids numbering at least 201 × 201. Increasing the number of grids to 401×401 and 801×801 was also tested. Only a 2% difference arises when the number of grids changed from 201 × 201 to 401 × 401. Thus, most computations were performed with the grids at 401 × 401. In order to apply the boundary condition (12b) at the exit of the reservoir (or at the entrance to the channel), we need to employ the asymptotic solution for the channel given in the previous section. In this application, we need to calculate the strength m, defined as

$$\mathbf{m} = -\int_{0}^{\pi} \cdot \frac{\partial \phi}{\partial \mathbf{r}} \, \mathop{,}_{d/2} d\eta \tag{14}$$

where $\partial \phi / \partial r$, the radial component of the electric field, can be obtained using the relation $\partial \phi / \partial r = \exp(-\xi) \partial \phi / \partial \xi$. We also used the second-order difference formula, i.e., (13), to evaluate $\partial \phi / \partial \xi$.

Thus, the computational procedure can be described as follows:

- (1) Set $\phi_b=0$ all over the reservoir outlet, $0 \le \eta \le \eta_c$ at $\xi = \xi_b$.
- (2) Solve the Laplace equation (1) with the boundary conditions (12a)-(12d).
- (3) Calculate m using (14).
- (4) Using this m value, update the function ϕ_b from (9) with the value of ζ computed from (7) for z_1 =iy, where y=Rsin η , at each grid point at the channel entrance (reservoir outlet) with $0 \le \eta \le \eta_c$.
- (5) Repeat (2)-(4) until convergence is attained.

Numerical Results

Figure 5 shows typical patterns of the equi-potential lines and the electric field lines that were obtained numerically. Overall, the patterns are physically relevant, indicating that the numerical method is correct. They also reveal clustering of both lines, not only near the exit of the domain, but also near the electrode surface. Such clustering adjacent to the electrode is more pronounced as the electrode size decreases. This means that the drop in potential across the reservoir should increase as the electrode size decreases. This figure can be compared with Figure 3, which was obtained from the asymptotic solution; the overall patterns are very similar, indicating that

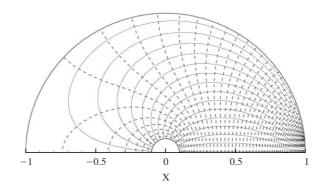


Figure 5. Numerical results of the equi-potential lines (dashed) and electric field lines (solid) where d=0.2 and w=0.2. The potential is 1.0 at the surface of the electrode and decreases at 0.02 increments.

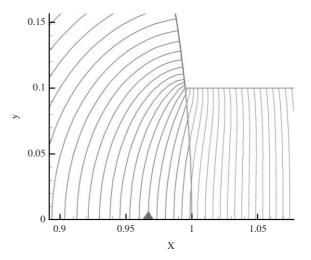


Figure 6. Patched pattern of the equi-potential lines given by the numerical solution for the circular reservoir (left-hand side domain; same parameter set as in Figure 3) and those given by the analytic solution for the exit channel (right-hand side domain). The potential line with a triangle mark on the x-axis has a potential of zero, with the value increasing on the left-hand side and decreasing on the right-hand side at increments.

neither the numerical nor analytical method is erroneous.

Figure 6 shows the patched pattern of the equipotential lines given by the finite volume method for the circular reservoir, and the patterns given by the complex function theory for the exit channel. Here, the vertical grid lines at the interface for the latter solutions are intentionally tilted slightly such that the interface line exactly fits that of the reservoir side. From this figure, we can see that the patching is almost complete. Furthermore, the error arising from such patching obviously decreases as the channel size

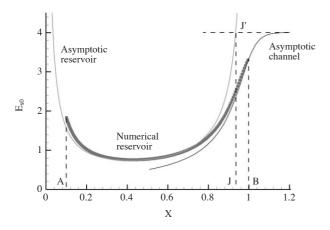


Figure 7. Distributions of E_{x0} , the x-component of the electric field along the line y=0, obtained by the asymptotic solution for the circular reservoir (upper solid line) and for the straight channel (lower solid line) with w=0.2, and that obtained by the numerical method (symbols) with d=w=0.2.

decreases.

Shown in Figure 7 are the distributions of E_{x0} , the x-component of the electric field along the line y=0 obtained by the asymptotic solution, applicable to the circular reservoir and to the straight channel, as well as the distribution obtained by the numerical method. We can see that the two asymptotic solutions are indeed asymptotic to the numerical solution on each side of the applicable region.

Effective Potential Difference and Electric Field

As mentioned previously, in order to calculate the electric field within the channel, we need to know the potentials at both ends. However, those values are not known *a priori* and we must attain a working formula to compute the effective potential difference or the electric field within the channel. In this section, we propose two formulae, one for the numerical method and the other for the analytical method.

We let the channel length be L. Further, we define ΔV_1 as the potential difference between the two channel ends and ΔV_2 as the potential difference between the anode and the end of the channel connected to the reservoir surrounding the anode; since we are considering a symmetric configuration, the potential difference is the same on the other side of the channel. Thus, the total difference in potential between the two electrodes is

$$\Delta V = \Delta V_1 + 2\Delta V_2 \tag{15}$$

The electric field within the channel is given by $E = \Delta V_1/L$, from which we have

$$\Delta V_1 = EL \tag{16}$$

The relation between ΔV_2 and E can be established using either the numerical result or by theoretical analysis. First, we considered the derivation of the formula given from the numerical result. We noticed that the electric current, E_w, across the full width of the channel should be the same as the corresponding one, i.e., the source strength across the reservoir, m= E_{w} . In the numerical calculation for the reservoir, we imposed a unit potential at the electrode surface and zero potential at point C, the intersection of the outer wall of the reservoir and the upper wall of the channel (see Figure 1 and Figure 4a). After numerical simulation of the Laplace equation for a certain set of d and w, we were left with the sink strength m_0 , and $\overline{\phi_0}$, the averaged potential at the outlet of the reservoir, i.e., the channel inlet section. Since the asymptotic solution for the potential is available at the channel entrance, we can write

$$\overline{\phi_0} = -0.0977 m_0$$

where the constant corresponds to the average potential $\overline{\phi_0}$ at m=1 obtained from the asymptotic solution for the channel. Then, since the electric potential at the electrode surface is maintained at 1 in the numerical simulation, we get $\Delta V_{20}=1-\overline{\phi_0}$. For an arbitrary value of m, we get $\Delta V_2=\Delta V_{20}(m/m_0)$. Applying m= E_w to this equation, we obtain

$$\Delta V_2 = \frac{(1+0.0977m_0)E_w}{m_0} \tag{17}$$

Substituting (16) and (17) into (15), we obtain

$$E = \frac{V}{L + \gamma 2R}$$
(18)

where the constant γ is

$$\gamma = \frac{1 + 0.0977 m_0}{m_0} \frac{w}{R}$$
(19)

18) can be considered a general equation for computation of the effective electric field E with V, L and R given. The constant γ is a key parameter that reflects the effect of reservoir design on E. If the space between the electrode and the channel inlet are replaced by a straight channel with the same width w, then the constant γ must become 1. The radius of the reservoir, R, shown in formulae (18) and (19), is not explicitly taken as 1, so that these formulae to be used in the general case when neither the channel length L nor the channel width w are scaled by R.

Now we turn to the theoretical method to determine the constant γ . Figure 7 shows the distributions of E_{x0} , the x-component of the electric field along the line y=0 for the case where d=w=0.2, obtained by the asymptotic solution for the circular reservoir and for the channel, together with the distribution given by the numerical method. The potential difference ΔV_2 between the electrode surface and the channel entrance, (17), corresponds to the area beneath the curve designated "numerical reservoir" in Figure 7:

$$\Delta V_2 = \int_{d/2}^{1} E_{x0} dx$$

We can obtain the equivalent from the relationship $\Delta V_2 = \phi_A^{num} - \phi_B^{num}$. If we use the asymptotic results, this may be computed from

$$\Delta V_2 = (\phi_A^{\text{res}} - \phi_J^{\text{res}}) + (\phi_J^{\text{cha}} - \phi_B^{\text{cha}})$$
(20)

where the first term is given from the "asymptotic reservoir" result and the second from the "asymptotic channel" result. Point J is determined by the requirement that the electric field computed from the asymptotic reservoir solution be the same as that obtained from the channel side, i.e., m/w. From the asymptotic reservoir solution, we get

$$\phi_{\rm A}^{\rm res} \cong -\frac{\rm m}{2\pi} \ln d$$

from (5) for small d. Next we also get

$$\phi_{\rm J}^{\rm res} \cong -\frac{\rm m}{2\pi} \ln \frac{\epsilon^2}{2}$$

from (5) for small ε defined as $\varepsilon = 1 - r_J$. Here the value of ε can be found from the condition of point J, which is

$$\cdot -\frac{\partial \phi}{\partial r} = \frac{m}{\eta = 0}$$

so that $\varepsilon = w/\pi$. Then,

$$\phi_{A}^{res} - \phi_{J}^{res} = -\frac{m}{2\pi} \ln\left[\frac{d}{2} \cdot \frac{w}{\pi}\right]^{2}$$
(21)

On the other hand, from the channel solution (8), we have

$$\phi_J^{cha} = \frac{m}{2\pi} \ln a$$

where a is the $-\zeta$ value given from (7) with $z_1 = -\varepsilon$. Then the equation for a is

$$2\sqrt{1+a} + \ln \left| \frac{\sqrt{1+a}-1}{\sqrt{1+a}+1} \right| - 2 = 0$$

Solving this equation, we get a=1.8349. Similarly, ϕ_B^{cha} can be obtained from

$$\phi_{\rm B}^{\rm cha} = \frac{m}{2\pi} \ln b$$

where b is the $-\zeta$ value from (7) when $z_1=0$. Solving the resultant equation, we obtain b=0.4392. Thus, we can write

$$\phi_{J}^{cha} - \phi_{B}^{cha} = \frac{m}{2\pi} \ln \cdot \frac{a}{b} , \qquad (22)$$

Substituting (21) and (22) into (20), we can derive the following:

$$\Delta V_2 = \frac{m}{2\pi} \left\{ \ln \cdot \frac{a}{b}, -\ln \left[\frac{d}{2} \cdot \frac{w}{\pi}, ^2 \right] \right\}$$

The constant γ to be used in (18) then becomes

$$\gamma = \frac{\mathrm{w}}{\pi \mathrm{R}} \left\{ 0.715 - \frac{1}{2} \ln \left[\frac{\mathrm{d}}{2\mathrm{R}} \cdot \frac{\mathrm{w}}{\pi \mathrm{R}}^2 \right] \right\}$$
(23)

where R is again included so that this formula can be applied to the general case when neither w nor d are scaled by R.

We found that this analytical result is best compared with that from the numerical results by replacing the constant 0.715 with another parameter β , so that

$$\gamma = \frac{w}{\pi R} \left\{ \beta - \frac{1}{2} \ln \left[\frac{d}{2R} \cdot \frac{w}{\pi R}^{2} \right] \right\}$$
(24)

The solid lines shown in Figure 8 are drawn with

$$\beta = 0.75 - 0.40 \, \text{d/R} \tag{25}$$

which is an empirical formula for the parameter β that gives the best agreement with the numerical results. As seen from this figure, formula (24) with β

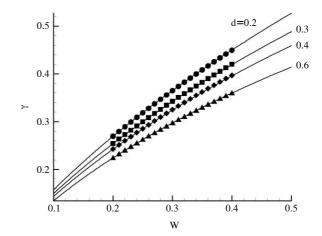


Figure 8. Effects of electrode diameter d and channel width on the value of γ used to calculate the electric field within the channel between two circular reservoirs. The symbols denote the numerical results, while the solid lines are given by formula (24) with (25).

given as (25) can be used for a wide range of parameter values of w/R and d/R.

It is also intuitively clear from (18), (24) and (25) that, when the reservoir radius, channel width and electrode diameter are kept constant, the values of β and γ are also kept constant; so, if only the channel length is decreased, the entrance effect is increased. On the other hand, decreasing d/R also increases the effect of the channel entrance on the electric field, as seen from (24) and (25). However, w/R has the reverse effect; that is, decreasing w/R decreases the channel entrance effect, as seen from (24). As a concrete example, consider a 10 mm-long and 0.1 mm-wide channel attached to circular reservoirs of radius 5 mm having electrodes of diameter 0.1mm. From equation (25), we obtain $\beta = 0.74$ and from (24), $\gamma = 0.052$; thus, we can estimate that there will be a 5.2% over-prediction when the conventional formula $E = \Lambda V/L$ is used.

Conclusions

In this paper, we presented numerical and analytical methods for solving the Laplace equation for the electric potential inside a space composed of a channel with two reservoirs attached to either end, each with an electrode at its center. A working formula was then derived from the solutions obtained for predicting the electric field inside the channel. The formula very accurately predicts the electric field for a wide range of parameter values. The entrance effect on the electric field within the channel increases when the channel length is decreased. The entrance effect also increases when the electrode diameter is decreased and channel width increased with reservoir size remaining unchanged.

Acknowledgements

This work was supported by the Korea Science and Engineering Foundation (KOSEF) through the National Research Laboratory Program funded by the Ministry of Science and Technology (No. 2005-01091).

References

- 1. Li, D. Electrokinetics in Microfluidics, Elsevier: 2004.
- Stone, H.A., Strook, A.D. & Ajdari, A. Engineering flows in small devices: Microfluidics toward a labon-a-chip. *Annu. Rev. Fluid Mech.* 36, 381-411 (2004).
- 3. Currie, I.G. Fundamental Mechanics of Fluids, McGraw-Hill Book Co.: 1974.
- Milne-Thomson, L.M. *Theoretical Hydrodynamics*, McMillan & Co. Ltd: 1968.
- 5. Ferziger, J.H. & Peric, M. Computational Methods for Fluid Dynamics, Springer: 2001.
- Suh, Y.K. & Yeo, C.H. Finite volume method with zonal-embedded grids for cylindrical coordinates. *Int. J. Num. Methods Fluids* **52**, 263-295 (2006).